Chiral Space Formed by (+)-(1*S*)-1,1′-Binaphthalene-2,2′-diyl Phosphate: Recognition of Aliphatic L-α-Amino Acids

by **Isao Fujii** and **Noriaki Hirayama***

Department of Biological Science and Technology, Tokai University, 317 Nishino, Numazu, Shizuoka 410-0321, Japan

(+)-(1*S*)-1,1′-Binaphthalene-2,2′-diyl hydrogen phosphate (bnppa) is one of the useful optical selectors. To disclose the molecular mechanism by which bnppa recognizes aliphatic L-α-amino acids and separates them by fractional crystallization, X-ray analyses of bnppa and of its salts with L-alanine, L-valine, L-norvaline, and L-norleucine have been undertaken. All the amino acids adopt energetically favorable conformations in the crystal structures. The conformations and the packing patterns of bnppa in these crystal structures are very similar. The bnppa molecules are packed in a specific way to form hydrophobic and hydrophilic layers that are well separated. Between bnppa molecules, at the interface of these hydrophobic and hydrophilic layers, a space with chirality is formed. This space, designated as chiral space, recognizes the optically active amino acids. The packing of bnppa is mainly governed by intermolecular CH $\cdots\pi$ interactions between naphthalene moieties. The chiral space is responsible for the molecular recognition by bnppa allowing fractional crystallization of the L-α-amino acids.

1. Introduction. – Optically active (1*S*)-(+)-1,1′-binaphthalene-2,2′-diyl hydrogen phosphate (bnppa; *Fig. 1*) has been known as a good optical resolution agent of amines [1][2]. Although bnppa is frequently employed in the resolution of synthetic intermediates of pharmaceuticals by fractional crystallization [3], molecular mechanisms by which bnppa recognizes these molecules have not yet been studied. Since bnppa is one of the effective chiral selectors, it is of great interest to study its molecular-recognition mechanism. Therefore, we started a systematic investigation with the aim to elucidate the molecular mechanisms by which bnppa recognizes the optically active amino acids.

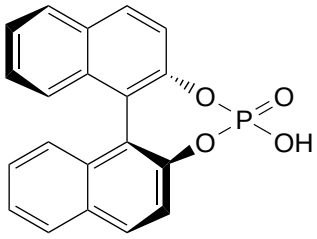

Fig. 1. *Chemical structure of bnppa*

In this study, we focused on the recognition of L-α-amino acids with aliphatic side chains of different sizes by bnppa by means of their crystallized salts. The salts between bnppa and L-alanine (Ala), L-valine (Val), L-norvaline (=(2*S*)-2-aminopentanoic

acid; Ape), and L-norleucine (=(2*S*)-2-aminohexanoic acid; Ahx) Ala·bnppa, Val·bnppa, Ape·bnppa, and Ahx·bnppa, as well as uncomplexed bnppa were examined by X-ray analyses to disclose the mode of interactions between the L-α-amino acids and bnppa. A molecular mechanism for the recognition of the L-α-amino acids with aliphatic side chains by bnppa is discussed.

2. Results and Discussion. – 2.1. *Molecular Structures of bnppa in Different Crystalline Fields.* bnppa Molecules adopt essentially the same structure in the five crystals submitted to X-ray analysis. An ORTEP-III [4] drawing of bnppa itself is shown in *Fig. 2*, and selected geometric parameters of bnppa in the different crystalline fields are tabulated in *Table 1*. Although the phosphate group is protonated in the bnppa crystal, it is dissociated in the crystals of the salts. Therefore, O(3)–P and O(4)–P distances in the uncomplexed bnppa crystal are significantly shorter and longer, respectively, than the corresponding values in the crystals of the salts. The lengths of other P–O bonds in the salts are also significantly different from the corresponding ones of free bnppa. The other bond lengths of bnppa are conserved, and no significant change due to formation of salts is observed.

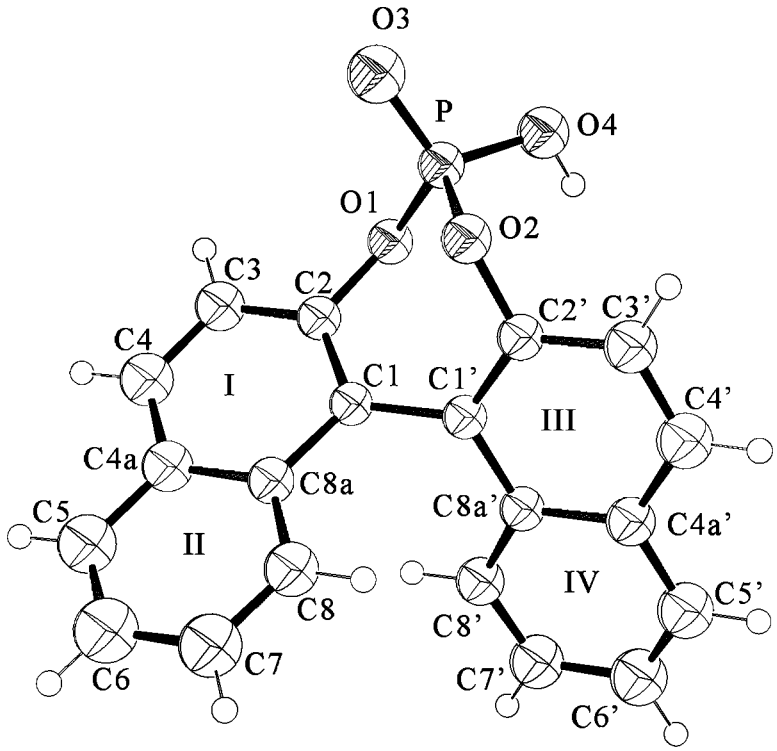

Fig. 2. *Crystal structure of bnppa with the atomic and ring numbering, drawn with ORTEP-III* [4]

Table 1. *Selected Geometric Parameters*

	Selected geometric parameters in bnppa					
	bnppa	Ala · bnppa	Val · bnppa	Ape · bnppa	Ahx · bnppa	[a])
Bond lengths [Å]						
C(1)–C(1′)	1.484(4)	1.485(3)	1.489(3)	1.492(5)	1.506(8)	1.503(9)
O(1)–C(2)	1.402(3)	1.392(2)	1.394(3)	1.395(4)	1.397(7)	1.393(7)
O(2)–C(2′)	1.403(4)	1.400(2)	1.397(3)	1.403(4)	1.404(7)	1.395(8)
P–O(1)	1.589(2)	1.596(2)	1.595(2)	1.598(2)	1.600(4)	1.597(4)
P–O(2)	1.584(2)	1.607(2)	1.600(2)	1.602(2)	1.610(4)	1.612(4)
P–O(3)	1.453(2)	1.474(2)	1.458(2)	1.470(2)	1.466(4)	1.471(5)
P–O(4)	1.525(2)	1.479(2)	1.495(2)	1.479(3)	1.477(5)	1.474(5)
Average of absolute values of torsion angles in benzene rings [°]						
Ring I	4.3(2)	4.4(1)	4.2(1)	4.6(2)	3.7(3)	4.1(3)
Ring II	1.2(3)	1.2(1)	1.0(2)	2.2(2)	2.5(4)	1.6(5)
Ring III	4.2(2)	5.2(1)	4.8(2)	3.4(2)	5.1(3)	4.4(3)
Ring IV	1.3(2)	1.1(1)	1.9(2)	1.1(2)	2.1(4)	2.1(4)
Selected torsion angles [°]						
C(8a)–C(1)–C(2)–C(3)	–7.8(5)	–7.8(3)	–7.3(4)	–7.3(5)	–5.6(9)	–6.7(9)
C(4a)–C(8a)–C(1)–C(2)	7.3(4)	7.3(3)	6.8(3)	8.0(5)	7.1(9)	8.1(9)
C(8a′)–C(1′)–C(2′)–C(3′)	–7.4(5)	–9.3(3)	–7.8(4)	–6.5(5)	–8.9(8)	–7.5(9)
C(4a′)–C(8a′)–C(1′)–C(2′)	7.4(4)	8.1(3)	9.1(4)	5.6(5)	8.6(8)	5.9(9)
Dihedral angles between naphthalene moieties [°]						
	61.1(1)	63.39(6)	61.9(1)	63.3(1)	62.0(2)	62.2(2)

	Selected torsion angles [°] in amino acids				
	Ala	Val	Ape	Ahx[a])	
O(1)–C–C(α)–C(β)[b])	129.1(2)	98.7(2)	112.2(4)	104.4(7)	131.0(9)
O(2)–C–C(α)–N[b])	–175.4(1)	157.7(2)	175.4(3)	168.7(5)	–178.3(5)
C–C(α)–C(β)–C(γ)		–56.9(3)	–178.4(4)	–179.5(5)	–62(1)
C–C(α)–C(β)–Cγ)		68.7(2)			
C(α)–C(β)–C(γ)–C(δ)			167.5(5)	178.2(6)	–148(1)
C(β)–C(γ)–C(δ)–C(ε)				–175.8(6)	–179(1)

[a]) The values for two crystallographically independent molecules are given. [b]) O(1) and O(2) denote carbonyl and hydroxy O-atoms, respectively.

Rings I and III of bnppa significantly deviate from planarity in all five crystals as indicated by the average of the absolute values of torsion angles in these rings (3.5–4.5° for ring I and 3.4–5.4° for ring III, see *Table 1*). The torsion angles C(8a)–C(1)–C(2)–C(3) and C(4a)–C(8a)–C(1)–C(2) in ring I and C(8a′)–C(1′)–C(2′)–C(3′) and C(4a′)–C(8a′)–C(1′)–C(2′) in ring III are especially large (*Table 1*). Rings II and IV are considered to be essentially planar.

Even though the naphthalene moieties are not necessarily planar as mentioned above, the dihedral angle between the least-squares planes of two naphthalene moieties should be an important geometrical characteristic of bnppa when it recognizes the amino acids. These angles are distributed in a narrow range between 61.1(1) and 63.39(6)° (*Table 1*). Although the angle in the free bnppa is the smallest, and the angle increases to some extent in the salts, the narrow range of the values indicates that the inherent structure of bnppa is not much deformed in salts. In other words, the packing

effects in the salts have only marginal influence on the conformation of the bnppa molecules.

2.2. *Conformations of the Amino Acids.* The carboxyl groups of the amino acid molecules are protonated in all of the salts. Therefore, the lengths of the two C–O bonds are significantly different. The amino groups are also protonated in the salts. The torsion angles relevant to the conformations of the amino acids are given in *Table 1*. The conformations of L-alanine and L-valine in the salts are very similar to those of their corresponding hydrochloride salts [5][6]. Although the conformation of L-norvaline is similar to that found in a complex between L-norvaline and D-norleucine [7], their torsion angles of O(1)–C–C(α)–C(β) and N–C(α)–C(β)–O(2) differ by more than 20°. The crystal structure of L-norleucine has not been disclosed so far and the present crystal structure is the first one. As indicated by the torsion angles in the *Table 1*, the aliphatic side chains of L-norvaline and L-norleucine (Ahx) adopt fully extended conformations. Since all amino acids in the salts take sterically favorable conformations, their conformations are not affected significantly in the crystal structures of the salts.

2.3. *Molecular Arrangement of bnppa Molecules in the Crystal.* The hydrophobic and hydrophilic regions of bnppa are well-separated in the molecule. These regions segregate in the crystal structure to form hydrophobic and hydrophilic layers as shown in *Fig. 3*. In the hydrophilic layer, the phosphate groups are connected to each other by H-bonds. The H-bond geometries are listed in *Table 2*. The naphthalene moieties aggregate into the hydrophobic layers. Although the packing is similar to a well-known herringbone structure [8], the packing pattern is more complex because both of the naphthalene moieties that are inclined to each other within a molecule are involved in the packing.

The packing is governed by CH$\cdots\pi$ interaction [9] between slightly positively charged H-atoms of one benzene ring and the electron-rich π-electron system of another benzene ring. As illustrated in *Fig. 4*, naphthalene moieties are packed together mainly by these CH$\cdots\pi$ interactions. The CH$\cdots\pi$ interaction can be estimated by using several geometric parameters. We focused on the geometric parameters tabulated in *Table 3*. They were calculated with the program PLATON [10]. Interactions with the distance H$\cdots$Cg and the angle γ being less than 3.4 Å and 20.0°, respectively, are considered as possible CH$\cdots\pi$ interactions in the present study.

Based on these criteria, three CH$\cdots\pi$ interactions are identified as illustrated in *Fig. 4*. The three interactions interconnect all bnppa molecules in the hydrophobic area. These are dominant intermolecular hydrophobic interactions, and no parallel stacking between benzene rings is observed in this crystal structure. The H-atoms at C(6) and C(7) interact with the benzene rings of the 2_1-screw-related molecules. On the other hand, the H-atom at C(6′) interacts with the benzene ring that is related by translation along the *a* axis.

2.4. *Packing Characteristics of the Crystal Structures of the Salts.* The crystal structure of Ala · bnppa is shown in *Fig. 5*. The naphthalene moieties of bnppa are packed together by the CH$\cdots\pi$ interactions to form hydrophobic layers. The packing pattern of bnppa in Ala · bnppa is very similar to that of uncomplexed bnppa. Thus, the geometric parameters of the CH$\cdots\pi$ interactions (*Table 3*) reveal essentially the same three

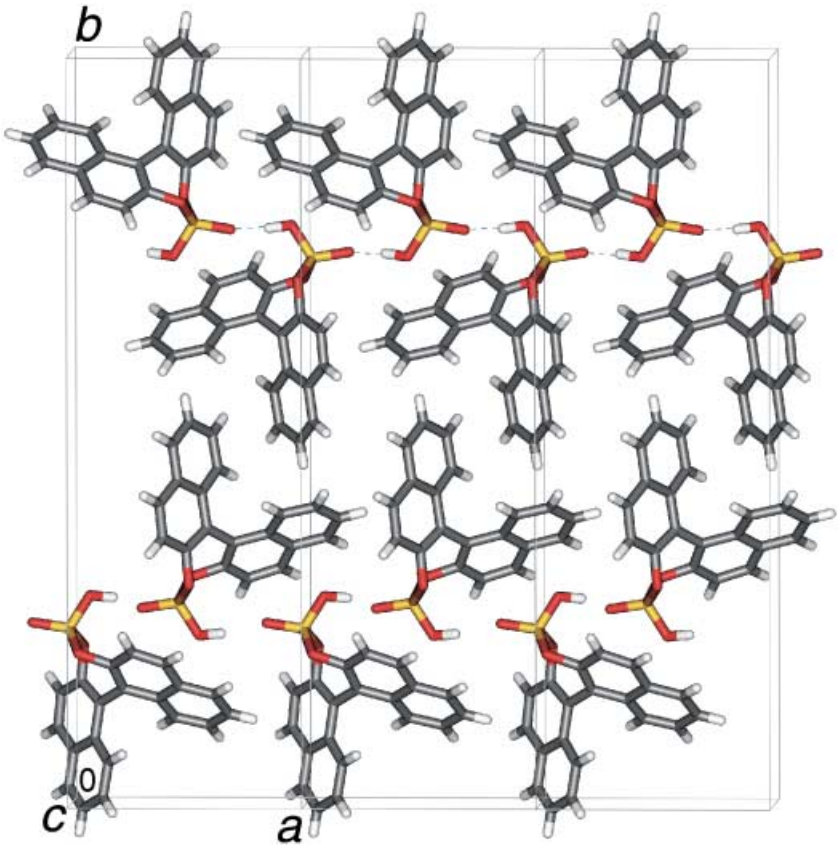

Fig. 3. *Crystal structure of bnppa viewed along the* c *axis, drawn with WebLab Viewer Pro* [11]. Dotted lines indicate H-bonds; P- and O-atoms are colored in yellow and red, respectively.

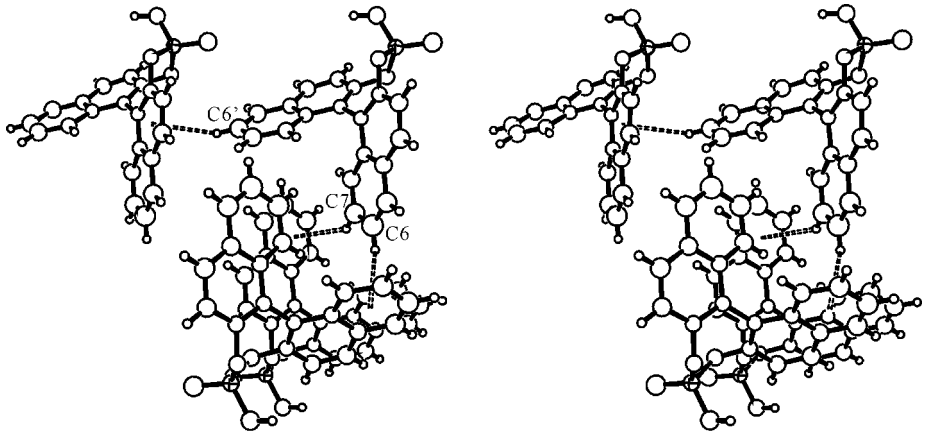

Fig. 4. *CH···π Interactions observed in the bnppa crystal.* Selected molecules are drawn (ORTEP-III [4]) for clarity.

Table 2. *Hydrogen Bonds*[a])

	Donor–H···Acceptor (symmetry code)	H···A [Å]	D···A [Å]	∢D–H···A [°]
bnppa	O(4)–H···O(3) (−1/2+*x*, −1/2−*y*, −1−*z*)	1.59	2.515(3)	174
L-Ala·bnppa	N(1a)–H···O(1a) (2−*x*, 1/2+*y*, −*z*)	2.53	2.904(2)	105
	N(1a)–H···O(4) (2−*x*, 1/2+*y*, 1−*z*)	2.37	2.930(2)	120
	N(1a)–H···O(1w) (*x*, 1+*y*, *z*)	1.88	2.724(3)	146
	N(1a)–H···O(3) (*x*, *y*, −1+*z*)	1.91	2.812(2)	145
	N(1a)–H···O(3) (2−*x*, 1/2+*y*, −*z*)	2.44	2.904(2)	107
	O(2a)–H···O(4) (2−*x*, −1/2+*y*, 1−*z*)	1.64	2.551(2)	178
	O(1w)–H···O(3) (*x*, *y*, −1+*z*)	1.81	2.736(3)	175
Val·bnppa	N(1v)–H···O(3) (1+*x*, *y*, *z*)	1.75	2.660(2)	175
	N(1v)–H···O(4) (1/2+*x*, 1/2−*y*, 1−*z*)	1.92	2.809(2)	171
	N(1v)–H···O(1v) (*x*, *y*, *z*)	2.27	2.676(2)	108
	N(1v)–H···O(1w) (*x*, *y*, 1+*z*)	2.09	2.834(4)	141
	O(2v)–H···O(4) (*x*, *y*, *z*)	1.82	2.620(2)	173
	O(1w)–H···O(1v) (1/2+*x*, 1/2−*y*, 1−*z*)	2.09	2.899(3)	167
Ape·bnppa	N(1ap)–H···O(1nv) (−*x*, −1/2+*y*, −2−*z*)	2.40	2.801(3)	108
	N(1ap)–H···O(2w) (*x*, −1+*y*, *z*)	1.98	2.859(3)	169
	N(1ap)–H···O(4) (−*x*, −1/2+*y*, −2−*z*)	1.92	2.786(3)	175
	O(1w)–H···O(2w) (*x*, *y*, *z*)	1.97	2.801(3)	171
	O(1w)–H···O(3) (*x*, 1+*y*, *z*)	2.04	2.818(3)	152
	O(2w)–H···O(3) (*x*, *y*, *z*)	2.04	2.829(3)	158
	O(2w)–H···O(1w) (−*x*, −1/2+*y*, −1−*z*)	1.91	2.735(3)	178
	O(2ap)–H···O(4) (−*x*, 1/2+*y*, −2−*z*)	1.76	2.577(3)	168
Ahx·bnppa	N(ah)(A)–H···O(4)(A) (*x*, *y*, −1+*z*)	2.03	2.845(5)	151
	N(ah)(A)–H···O(1w) (*x*, *y*, −1+*z*)	2.04	2.875(5)	157
	N(ah)(A)–H···O(1ah)(B) (*x*, *y*, −1+*z*)	2.50	2.886(5)	107
	N(ah)(A)–H···O(1ah)(B) (*x*, *y*, −1+*z*)	2.34	2.886(5)	120
	N(ah)(B)–H···O(2w) (*x*, *y*, *z*)	1.98	2.858(5)	170
	N(ah)(B)–H···O(1ar)(A) (*x*, *y*, *z*)	2.25	2.736(5)	115
	N(ah)(B)–H···O(4)(A) (*x*, *y*, *z*)	2.57	3.395(5)	157
	N(ah)(B)–H···O(4)(B) (*x*, *y*, *z*)	1.97	2.853(6)	169
	O(1w)–H···O(4w) (1+*x*, *y*, *z*)	1.97	2.764(5)	161
	O(1w)–H···O(3)(B) (*x*, *y*, *z*)	2.11	2.824(5)	144
	O(2w)–H···O(3)(A) (*x*, *y*, −1+*z*)	2.13	2.888(5)	154
	O(2w)–H···O(3w) (*x*, *y*, *z*)	1.91	2.701(6)	162
	O(3w)–H···O(3)(B) (−1+*x*, *y*, *z*)	2.30	2.853(6)	126
	O(4w)–H···O(3)(A) (*x*, *y*, *z*)	2.11	2.797(5)	139

[a]) A and D denote H-bond acceptor and donor, respectively. Crystallographically independent molecules in Ahx·bnppa are distinguished by A and B in parentheses. Descriptors a, v, ap, ah, and w denote Ala, Val, Ape, Ahx, and H_2O molecules, respectively.

CH···π interactions, indicating that the bnppa molecules of Ala·bnppa related by a 2_1 screw axis, are packed together by the CH···π interactions to form columns along the *b* axis, and the columns are further interconnected by the third CH···π interactions to form a hydrophobic layer along the *c* axis. L-Alanine and H_2O molecules in an asymmetric unit are located in the hydrophilic layer. All possible H-bond donors and acceptors of the phosphate groups, and the L-alanine and H_2O molecules are involved in H-bonding. These H-bonded molecules form columns around the 2_1 screw axis along the *b* axis. The amino group of L-alanine is H-bonded to the phosphate group.

Table 3. *Possible Intermolecular CH···π Interactions*

	C–H···ring (symmetry code)	H···Cg [Å][a])	C···Cg [Å]	∢C–H···Cg [°]	Perp(H···ring) [Å][a])	γ [°][a])
Between naphthalene moieties						
bnppa	C(6)–H···ring IV (−3/2−x, −y, −1/2+z)	2.95	3.74	142	2.92	8.2
	C(7)–H···ring II (−3/2−x, −y, 1/2+z)	3.06	3.83	139	3.01	10.4
	C(6′)–H···ring I (−1+x, y, z)	2.91	3.67	138	2.90	4.8
Ala·bnppa	C(6)–H···ring IV (1−x, 1/2+y, 1−z)	2.90	3.70	142	2.86	9.6
	C(7)–H···ring II (1−x, −1/2+y, 1−z)	3.05	3.81	138	3.04	5.9
	C(6′)–H···ring I (x, y, −1+z)	3.07	3.76	131	2.96	15.3
Val·bnppa	C(6)–H···ring IV (−1/2−x, −y, −1/2+z)	3.06	3.84	140	3.03	7.8
	C(7)–H···ring II (−1/2−x, −y, 1/2+z)	2.95	3.71	139	2.93	6.5
Ape·bnppa	C(6′)–H···ring IV (−1−x, −1/2+y, −2−z)	2.98	3.79	145	2.97	5.4
	C(7′)–H···ring II (−1−x, 1/2+y, −2−z)	2.95	3.69	135	2.95	0.8
Ahx·bnppa[b])	C(6)–H(A)···ring II(B) (1−x, 1/2+y, 2−z)	2.98	3.90	167	2.92	11.1
	C(7)–H(A)···ring IV(B) (1−x, 1/2+y, 1−z)	3.06	3.83	139	3.05	4.3
	C(6′)–H(B)···ring IV(A) (1−x, −1/2+y, 1−z)	2.77	3.62	150	2.75	7.1
	C(7′)–H(B)···ring II(A) (1−x, −1/2+y, 2−z)	3.12	3.90	140	3.04	12.7
Between benzene rings and aliphatic side chains of L-amino acids						
Ala·bnppa	C(β)–H···ring III (x, y, z)	3.25	3.67	109	3.18	12
Val·bnppa	C(δ)–H···ring IV (x, y, z)	3.22	3.85	126	3.12	14
Ape·bnppa	C(δ)–H···ring IV (−x, −1/2+y, −1−z)	2.78	3.65	153	2.66	17
Ahx·bnppa[b])	C(ε)–H(A)···ring I(A) (1+x, y, −1+z)	3.14	3.70	119	3.06	13
	C(δ)–H(B)···ring I(B) (−1+x, y, z)	2.75	3.65	171	2.61	18
	C(ε)–H(B)···ring III(B) (x, y, z)	2.94	3.61	129	2.86	13

[a]) Cg, Perp(H···ring), and γ denote the center of benzene ring, the perpendicular distance of the H-atom on the pertinent ring, and $\cos^{-1}$(Perp(H···ring)/H···Cg), respectively. [b]) Crystallographically independent molecules in the complex of Ahx·bnppa are distinguished by A and B in the parentheses.

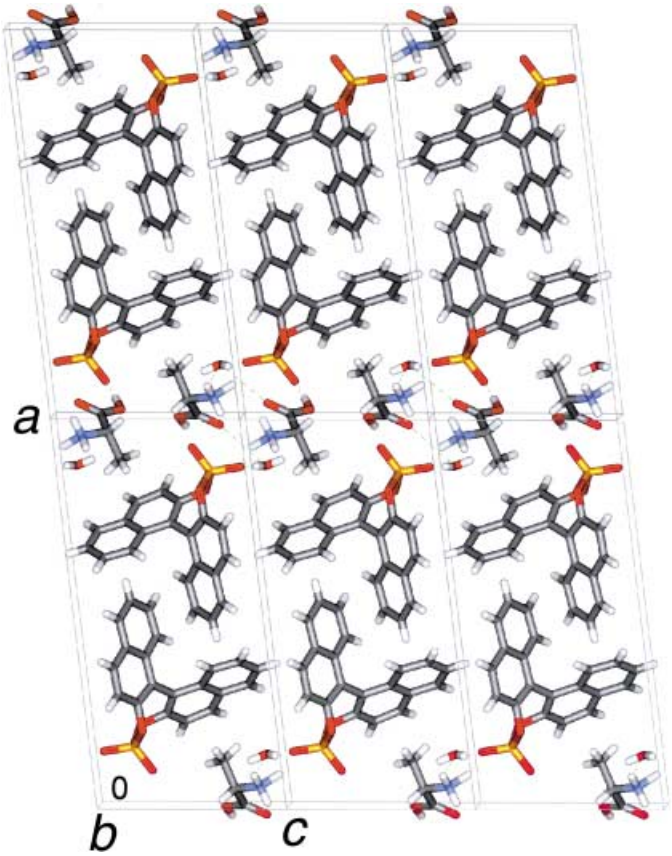

Fig. 5. *Crystal structure of Ala · bnppa viewed along the* b *axis, drawn with WebLab Viewer Pro* [11]. Dotted lines indicate H-bonds; P-, O-, and N-atoms are colored in yellow, red, and blue, respectively.

The crystal structure of Val · bnppa is shown in *Fig. 6*. The bnppa molecules are connected *via* the CH $\cdots\pi$ interactions by the 2_1 screw along the *c* axis. This interaction pattern is very similar to those observed in the crystal structures of bnppa and Ala · bnppa (*cf.* geometric parameters in *Table 3*). The distance between the bnppa molecules related by the translation along the *a* axis, however, is increased due to formation of salts with L-valine, whose side chain is bulkier than that of L-alanine. Accordingly, the third CH $\cdots\pi$ interaction that is observed in the crystals of bnppa and Ala · bnppa is no longer present in the crystal of Val · bnppa. The C(6′)–H, however, still points to the center of the pertinent flanking benzene ring. It indicates that *Van der Waals* interactions instead of CH $\cdots\pi$ interactions still contribute to the packing of bnppa molecules along the *a* axis in this case. The hydrophilic moiety of L-valine and the H_2O molecules are located in the well-separated hydrophilic layers. They, together with the phosphate groups, form an extensive H-bond network. The H-bonds along the *a* axis form an infinite H-bond network. All possible H-bond acceptors and donors are

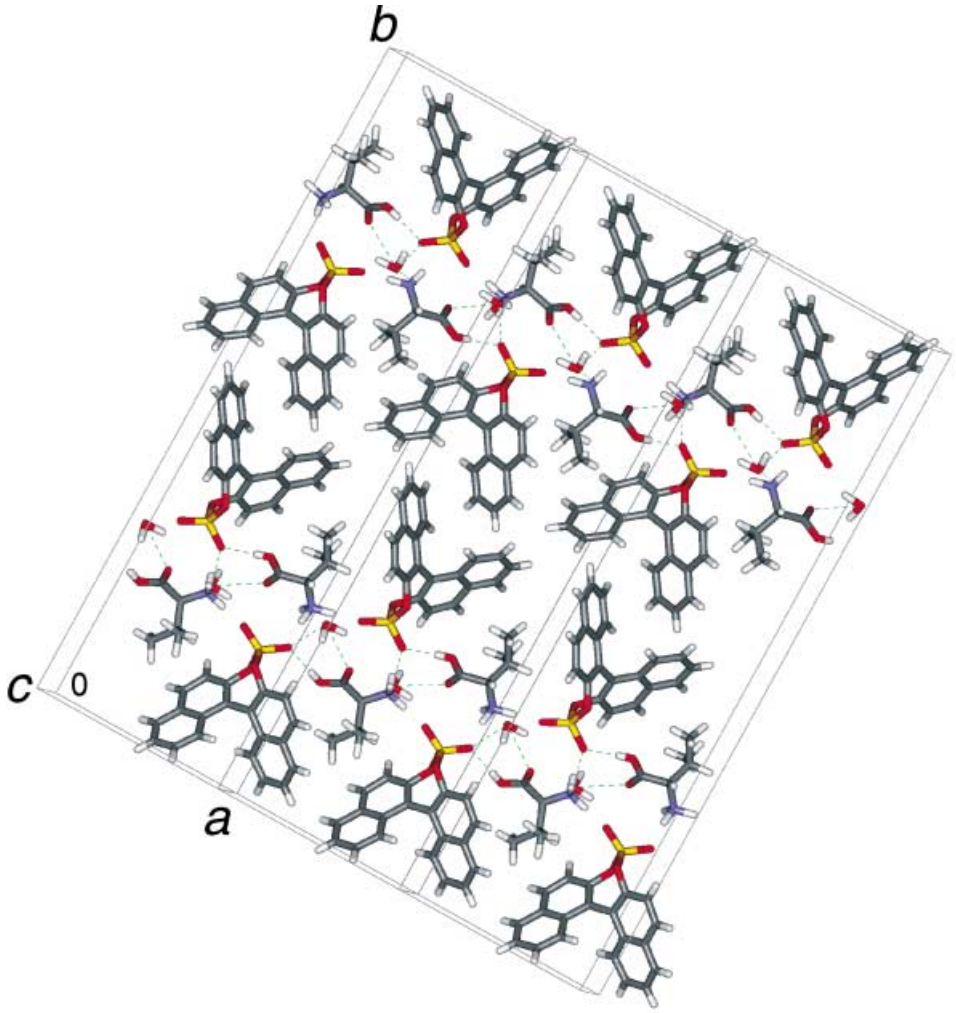

Fig. 6. *Crystal structure of Val · bnppa viewed along the* c *axis, drawn with WebLab Viewer Pro* [11]. Dotted lines indicate H-bonds; P-, O-, and N-atoms are colored in yellow, red, and blue, respectively.

engaged in the H-bond formation. The amino group of the amino acid is H-bonded to the phosphate group.

The crystal structure of Ape · bnppa is shown in *Fig. 7*. The 2_1-screw-related bnppa molecules form the hydrophobic column parallel to the *c* axis by the CH$\cdots\pi$ interactions, just like in the three crystal structures so far described (*cf.* geometric parameters in *Table 3*). The third CH$\cdots\pi$ interaction observed in bnppa and Ala · bnppa crystals is missing. Since the C(6)–H is pointing towards ring II of the next neighboring bnppa molecule, bnppa molecules are still interconnected through *Van der Waals* interactions at this region, just like in the Val · bnppa crystal. There are two H_2O molecules in an asymmetric unit and they, together with L-norvaline molecules and the

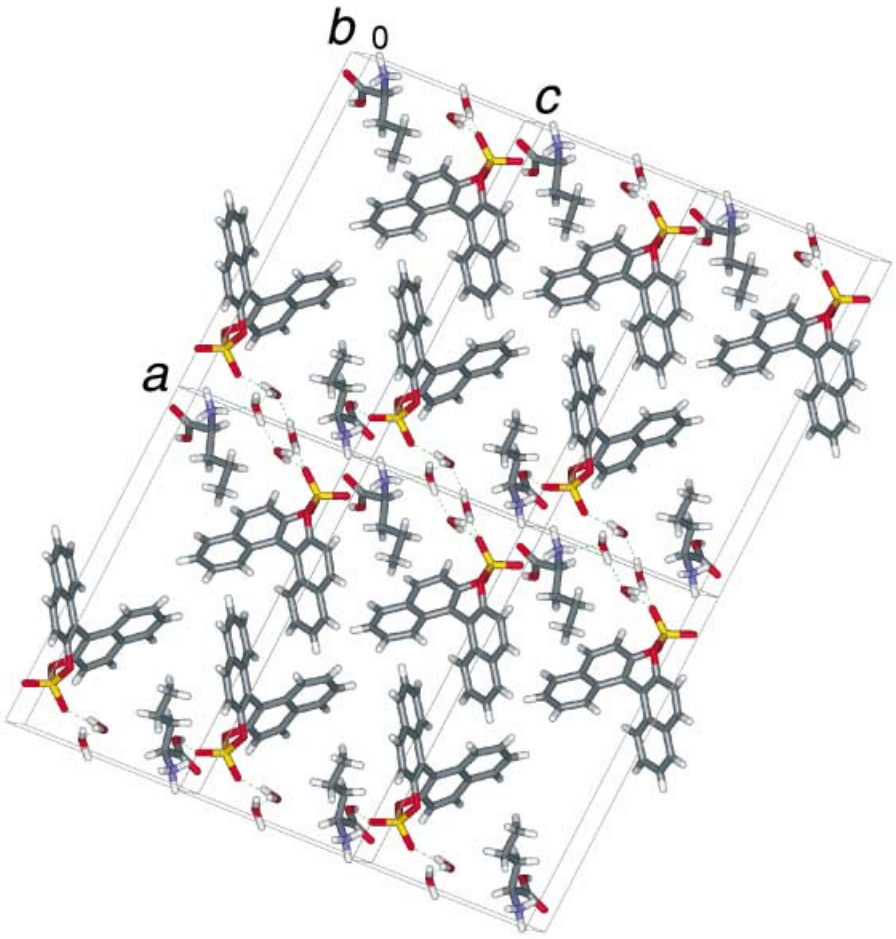

Fig. 7. *Crystal structure of Ape · bnppa viewed along the* b *axis, drawn with WebLab Viewer Pro* [11]. Dotted lines indicate H-bonds; P-, O-, and N-atoms are colored in yellow, red, and blue, respectively.

phosphate groups, form hydrophilic layers by an extensive H-bond network along the *c* axis. All the possible H-bond acceptors and donors are involved in H-bond formation. The amino group of the amino acid is H-bonded to the phosphate group. Secluded bnppa molecules along the *c* axis also develop a void in the hydrophilic layer that should be occupied by an additional H_2O molecule to maintain the stability of the crystal.

Although there are two bnppa, two L-norleucine, and two H_2O molecules in an asymmetric unit of the crystal of Ahx · bnppa, the packing pattern of this crystal is very similar to that of Ape · bnppa (*Fig. 8*). The phosphate group, and L-norleucine and H_2O molecules are engaged in a H-bond network along the *a* axis. The naphthalene moieties of both of the two crystallographically independent bnppa molecules are packed together by the CH $\cdots$ π interactions by a 2_1 screw axis along the *c* axis. The geometric

parameters of these CH$\cdots\pi$ interactions are given in *Table 3*. These values are very similar to those of other salts. The bnppa molecules related by the translation along the *a* axis are not interconnected by the CH$\cdots\pi$ interactions, but they are bound by *Van der Waals* interactions.

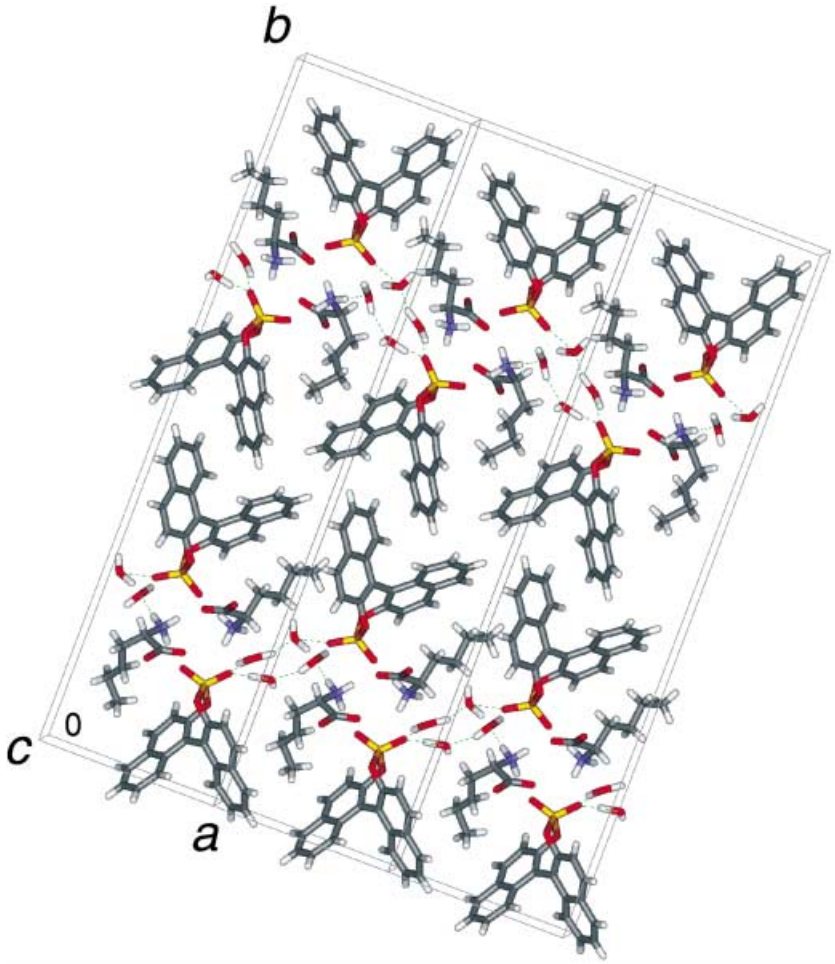

Fig. 8. *Crystal structure of Ahx·bnppa viewed along the* c *axis, drawn with WebLab Viewer Pro* [11]. Dotted lines indicate H-bonds; P-, O-, and N-atoms are colored in yellow, red, and blue, respectively.

2.5. *Recognition Mechanism of Aliphatic* L-*α-Amino Acids by bnppa*. As revealed in the five crystal structures mentioned above, bnppa molecules share essentially the same packing pattern in these different crystalline fields. The bnppa molecules highly tend to form chains by the CH$\cdots\pi$ interactions between the naphthalene moieties of the adjoining bnppa molecules. These interactions form 2_1 helix chains along the shortest crystallographic axes, *e.g.*, 5.994, 6.296, 6.094, 6.536, and 6.449 Å in the crystals of bnppa, Ala·bnppa, Val·bnppa, Ape·bnppa, and Ahx·bnppa, respectively. The bnppa

molecules in the neighboring chains are also likely to be interconnected to each other by the CH $\cdots\pi$ interactions. The interactions are formed between the molecules related by the translation along the second shortest crystallographic axes. In the salts of the amino acids with larger side chains, the latter CH $\cdots\pi$ interactions are weakened and replaced by usual *Van der Waals* interactions.

To illustrate the space where the amino acids are recognized by bnppa molecules, part of the crystal structure of Ape · bnppa is shown in *Fig. 9*, *a*. The bnppa molecules related by the translation along a crystallographic axis form a space between them where chiral amino acids can be recognized. Hereafter, we use a term 'chiral space' to describe this particular space that is formed between chiral molecules and holds a chirality. *Fig. 9*, *b*, clearly shows how this chiral space is used to recognize the optically active amino acid. The chiral space shaped by bnppa molecules may play a decisive role in the molecular recognition of the amino acids. Possible CH $\cdots\pi$ interactions between aliphatic side chains of the amino acids and the benzene rings of bnppa are also listed in *Table 3*. Judging from these geometric parameters, the CH $\cdots\pi$ interactions may significantly contribute to the molecular recognition of optically active amino acids in the chiral space. The inherent character of bnppa molecules to aggregate in a specific way to build the chiral space among them underlies the molecular recognition by bnppa.

To accommodate larger side chains, however, the bnppa molecules can be shifted along the crystallographic axis to some extent. According to this shift, certain gaps are generated in the hydrophilic layers. The gaps are filled with H_2O molecules to stabilize the crystal structures. The flexible and smooth change of intermolecular interactions along the crystallographic axes from the CH $\cdots\pi$ interactions to usual *Van der Waals* interactions makes it possible that the chiral space accommodates aliphatic amino acids of various sizes with relative ease. Under such elastic conditions, the aliphatic side chains could adopt relaxed conformations in the chiral spaces.

As shown in *Fig. 9*, *a*, phosphate groups are located at the entrance of the chiral space to tether protonated amino groups of L-amino acids by H-bonds. The geometric parameters of these H-bonds (*cf. Table 2*) show that this H-bond between phosphate and protonated amino groups are observed in all the crystal structures determined in the present study. It is obvious that the phosphate group is one of the essential parts of the chiral space, and the H-bond also plays an important role in molecular recognition.

3. Conclusions. – The naphthalene moieties of bnppa pack together in a very specific way through the CH $\cdots\pi$ interactions in the crystals. This characteristic mode of interactions is essentially maintained in the five different crystal structures of bnppa itself (*Figs. 3* and *4*), and salts of bnppa with four L-amino acids with different aliphatic side chains (*Figs. 5–8*). These results indicate that bnppa has a marked tendency to adopt this particular packing structure. When bnppa molecules are aligned to pack in this way, a space is generated between bnppa molecules. The space surrounded by naphthalene moieties and phosphate groups is chiral because of the atropisomerism of bnppa. In this chiral space, the L-amino acids are recognized. Since the shape of this chiral space is conserved in the five crystals structures, the chiral space should play an important role in the recognition of the L-amino acid molecules and the crystallization of the salts. The present study has shown that molecular recognition and fractional

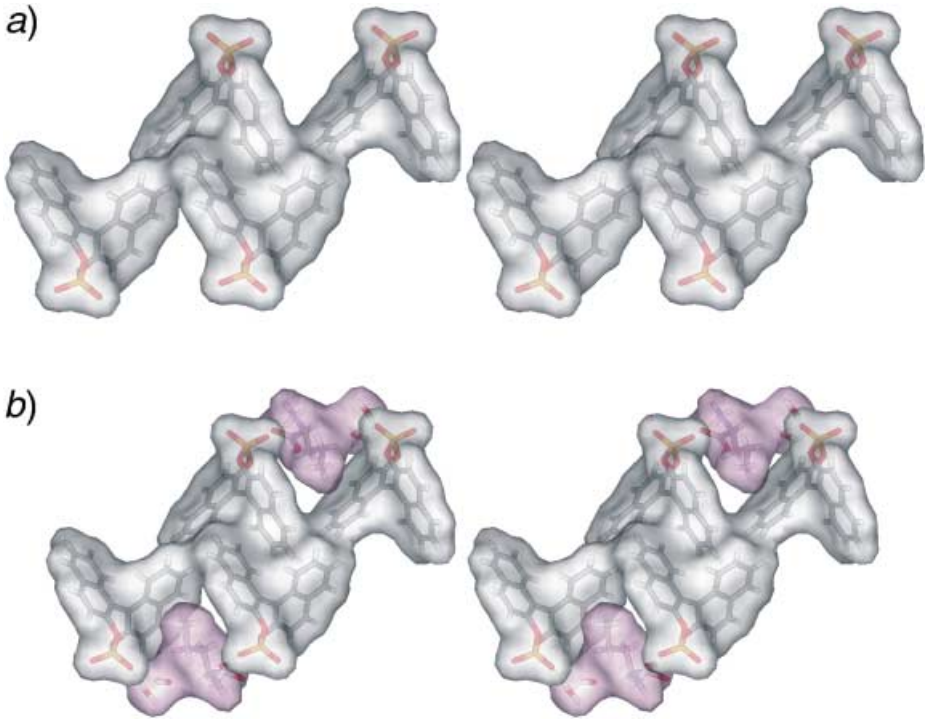

Fig. 9. a *Chiral space formed by bnppa molecules in the crystal of Ape · bnppa drawn with the program WebLab Viewer Pro* [11] (the solvent-accessible surface is drawn to illustrate the characteristic shape of the chiral space, and Ape and H_2O molecules are omitted to reveal the landscape of the chiral space). b) *The chiral space occupied by Ape and H_2O molecules.*

crystallization of L-α-amino acids with aliphatic side chains by bnppa is based on the strong tendency of bnppa to form this chiral space.

Experimental Part

1. *Crystallization and X-Ray Diffraction Experiments*[1]). The bnppa and L-amino acids were purchased from *Tokyo Chemical Industry Co. Ltd.* and *Sigma Chemical Co. Ltd.*, resp. They were used without further purification. Crystals of bnppa were obtained by slow evaporation of the acetone soln.

To obtain crystals of the salts between bnppa and the amino acids, equimolar quantities of bnppa and the amino acids were dissolved in various solvents (see *Table 4*). The solns. were stored at r.t. ($293 \pm 1°$), and crystals were grown by slow evaporation. Single crystals of salts between bnppa and L-alanine, L-valine, L-norvaline, and L-norleucine were successfully obtained.

Salts with L-leucine and L-isoleucine have not been crystallized in spite of the extensive attempts with various solvent systems so far. In these cases, only bnppa was fractionally crystallized from the solns.

---

[1]) Crystallographic data (excluding structure factors) for the structures reported in this paper have been deposited with the *Cambridge Crystallographic Data Centre* as deposition No. CCDC-182411 – CCDC-182415. Copies of the data can be obtained, free of charge, on application to the CCDC, 23 Union Road, Cambridge CB2 1EZ, UK (fax: +44(1223)33 6033; e-mail: deposit@ccdc.cam.ac.uk).

Table 4. *Crystallographic Data*

	bnppa[a])	Ala · bnppa	Val · bnppa	Ape · bnppa	Ahx · bnppa
Formula	$C_{20}H_{13}O_4P$	$C_{20}H_{12}O_4P \cdot C_3H_8NO_2 \cdot H_2O$	$C_{20}H_{12}O_4P \cdot C_5H_{12}NO_2 \cdot H_2O$	$C_{20}H_{12}O_4P \cdot C_5H_{12}NO_2 \cdot 2\,H_2O$	$C_{20}H_{12}O_4P \cdot C_6H_{13}NO_2 \cdot 2\,H_2O$
Solvent	ethylacetate	ethylacetate	acetone	EtOH	EtOH
Space group	$P2_12_12_1$	$P2_1$	$P2_12_12_1$	$P2_1$	$P2_1$
Crystal system	orthorhombic	monoclinic	orthorhombic	monoclinic	monoclinic
Formula weight	348.29	455.39	483.44	501.47	514.49
a [Å]	9.1899(7)	19.171(2)	10.7790(7)	19.663(1)	10.0983(7)
b [Å]	29.465(3)	6.2961(3)	37.600(2)	6.5361(5)	39.593(3)
c [Å]	5.9936(4)	9.1679(7)	6.0942(5)	9.845(2)	6.4488(6)
β [°]		96.743(6)	95.923(8)	92.599(6)	
V [Å^3]	1622.9(2)	1099.0(1)	2470.0(3)	1258.5(2)	2575.7(3)
Z	4	2	4	2	4
D_{calc} [g cm^{-1}]	1.425	1.376	1.300	1.323	1.327
μ [mm^{-1}]	1.704	1.506	1.370	1.393	1.376
$F(000)$	720	476	1016	528	1084
T [K]	293(1)	293(1)	293(1)	293(1)	293(1)
$2\theta_{(max)}$ [°]	73.99	74.01	74.03	73.99	74.04
Total reflections measured	3714	2520	2962	2880	5791
Symmetry-independent reflections	2052	2445	2928	2800	5412
Observed reflections ($F^2 > 3 \cdot (F^2)$)	1833	2349	2585	2459	3632
$R(F^2 > 3 \cdot (F^2))$					
R[b])	0.0395	0.0317	0.0424	0.0431	0.0516
wR[c])	0.1104	0.0991	0.1224	0.1248	0.1268
Goodness-of-fit	1.826	1.859	1.582	1.699	1.801
Final Δ_{max}/σ	0.01	0.01	0.05	0.01	0.05
$\Delta\rho$(max; min) [e/Å^{-3}]	0.26; −0.35	0.29; −0.28	0.38; −0.29	0.39; −0.24	0.54; −0.38

[a]) bnppa denotes (+)-(1*S*)-bnppa. [b]) $R = \Sigma\,||F_o| - |F_c||\,/\,\Sigma\,|F_o|$. [c]) $wR = \Sigma\{w(F_o^2 - F_c^2)^2 / \Sigma w(F_o^2)^2\}^{1/2}$, $w = 1/[\sigma^2(F_o^2) + (0.045P)^2]$, where $P = (\mathrm{Max}(F_o^2, 0) + 2F_c^2)/3$.

Crystal data of bnppa and its salts with the L-amino acids were collected by means of an *Enraf-Nonius CAD4-Turbo* diffractometer with graphite-monochromated CuK_α radiation ($\lambda = 1.54184$ Å). *Lorentz* and polarization corrections were applied to the data. No absorption corrections were made. Crystallographic data are summarized in *Table 4*.

2. *Structure Solution and Refinement*[1]). All structures were solved by direct methods. The program SAPI [12] was used to solve the crystal structures of bnppa and Ala · bnppa. The crystal structures of Val · bnppa, Ape · bnppa, and Ahx · bnppa were solved by DIRDIF [13], MULTAN88 [14], and SIR88 [15], resp. All non-H-atoms were refined anisotropically by the full-matrix least-squares method on F^2. The H-atoms attached to carboxy, hydroxy, and phosphate O-atoms were located by difference *Fourier* syntheses. Although the positions of H-atoms of H_2O molecules were deduced from difference *Fourier* syntheses, the positions of the H-atoms that are not involved in H-bonds are not certain. The positions of other H-atoms were geometrically calculated. All the H-atoms were fixed during the least-squares calculations. The absolute structure was assigned in each case by using the known chirality of the molecule. Crystallographic calculations were performed with the software package teXsan [16]. A summary of the structure refinements is given in *Table 5*.

REFERENCES

[1] W. Arnold, J. J. Daly, R. Imhof, E. Kyburz, *Tetrahedron Lett*. **1983**, *24*, 343.
[2] S. H. Wilen, J. Z. Qi, P. G. Williard, *J. Org. Chem*. **1991**, *56*, 485.
[3] Y. Kuge, K. Shioga, T. Sugaya, S. Tomioka, *Biosci. Biotechnol. Biochem.* **1993**, *57*, 1157.
[4] M. N. Burnett, C. K. Johnson, 'ORTEP-III: Oak Ridge Thermal Ellipsoid Plot Program for Crystal Structure Illustration', Oak Ridge National Laboratory Report ORNL-6895, 1996.
[5] B. di Blasio, V. Pavone, C. Pedone, *Cryst. Struct. Commun*. **1977**, *6*, 745.
[6] O. Ando, T. Ashida, Y. Sasada, M. Kakudo, *Acta Crystallogr*. **1967**, *23*, 172.
[7] B. Dalhus, C. H. Gorbitz, *Acta Crystallogr., Sect. C* **1999**, *55*, 1105.
[8] J. M. Robertson, *Proc. Roy. Soc. (London)*, **1951**, *A207*, 101.
[9] Y. Umezawa, S. Tsuboyama, K. Honda, J. Uzawa, M. Nishio, *Bull. Chem. Soc. Jpn*. **1998**, *71*, 1207.
[10] A. L. Spek, *Acta Crystallogr., Sect. A* **1990**, *46*, C-34.
[11] 'WeLab ViewerPro', Version 4.0, Molecular Simulations Inc., San Diego, 2000.
[12] Fan Hai-Fu, 'R-SAPI88: Structure Analysis Programs with Intelligent Control', Rigaku Corporation, Tokyo, 1988.
[13] V. Parthasarathi, P. T. Beurskens, H. J. B. Slot, *Acta Crystallogr., Sect. A* **1983**, *39*, 860.
[14] T. Debaerdemaeker, C. Tate, M. M. Woolfson, *Acta Crystallogr., Sect. A* **1985**, *41*, 286.
[15] M. C. Burla, M. Camalli, G. Cascarano, C. Giacovazzo, G. Polidori, R. Spagna, D. J. Viterbo, *J. Appl. Crystallogr.* **1989**, *22*, 389.
[16] 'teXsan: Single Crystal Structure Analysis Software', Version 1.10, Molecular Structure Corporation, The Woodlands, Texas, 1999.

Received April 2, 2002